Bioorganic Chemistry 91 (2019) 103156

Contents lists available at ScienceDirect

Bioorganic Chemistry

journal homepage: www.elsevier.com/locate/bioorg

Synthesis, in silico and in vitro studies of new 1,4-dihydropiridine derivatives for antitumor and P-glycoprotein inhibitory activity

Shirin Mollazadeh[a,b], Amirhossein Sahebkar[b,c,d], Fatemeh Kalalinia[b], Javad Behravan[a,b], Farzin Hadizadeh[a,b,*]

[a] Department of Medicinal Chemistry, School of Pharmacy, Mashhad University of Medical Sciences, Mashhad, Iran
[b] Biotechnology Research Center, Pharmaceutical Technology Institute, Mashhad University of Medical Sciences, Mashhad, Iran
[c] Neurogenic Inflammation Research Center, Mashhad University of Medical Sciences, Mashhad, Iran
[d] School of Pharmacy, Mashhad University of Medical Sciences, Mashhad, Iran

ARTICLE INFO

Keywords:
Apoptosis
Cytotoxicity
1,4-Dihydropyridine
Efflux assay
Molecular dynamic
P-glycoprotein

ABSTRACT

P-glycoprotein (P-gp) is one of the cell membrane pumps which mediate the efflux of molecules such as anticancer drugs to the extracellular matrix of tumor cells. P_gp is a member of the ATP-binding cassette (ABC) transporter family that is implicated in cancer multidrug resistance (MDR). Since MDR is a contributor to cancer chemotherapy failure, modulation of efflux pumps is a viable therapeutic strategy. In this study, new synthetic 1,4 dihydropiridine (DHP) derivatives containing thiophenyl substitution were tested as inhibitors of P-gp. Efflux assay was conducted to evaluate the intracellular accumulation of Rhodamine123 (Rh123) as a pump substrate. MTT assay, cell cycle analysis and in silico methods were also examined. Flow cytometric analysis revealed that synthetic DHP derivatives (15 μM) increased intracellular concentration of the substrate by 2–3 folds compared with verapamil as a standard P-gp inhibitor. MTT assay on EPG85-257P and its drug-resistant EPG85-257RDB cell line revealed antitumor effects (30–45%) for new DHP derivatives at 15 μM following 72 h incubation. However, MTT test on normal cell line showed negligible toxic effects. Finally combination of synthetic derivatives with doxorubicin showed that these compounds decrease IC50 of doxorubicin in resistant cell lines from 9 to 1.5 μM. Sub-G1 peak-related apoptotic cells showed a stronger effect of synthetic compounds at 5 μM compared with verapamil. Molecular dynamic results showed a high binding affinity between DHP derivative and protein at drug binding site. Findings of these biological tests indicated the antitumor activity and P-gp inhibitory effects of new 1,4-DHP derivatives.

1. Introduction

One of the most important factors involved in chemotherapy failure is multi-drug resistance. The main cause of MDR is overexpression of the ABC transporters such as P-glycoprotein. This protein pumps anticancer drugs out of the tumor cell [1]. Transportation of anticancer drugs *via* P-gp is responsible for reduced drug accumulation in tumor cells, thereby promoting resistance to chemotherapy [2]. P-gp efflux pump is distributed and expressed in the intestinal epithelium, liver, kidney, blood–brain barrier and other tissues [3]. Several cellular signaling pathways involving a multitude of transcription factors and also several microRNAs have been reported to regulate the sensitivity of cells to anticancer drugs by controlling the expression and function of P-gps [4,5]. The function of P-gp in the presence of different ligands (substrate or inhibitor) is stimulated as conformational changes associated with closeness of two NBDs and ATP hydrolysis [6,7]. Inhibition of ABC transporters, particularly P-gps, has been suggested as a promising strategy to increase the efficacy of anticancer agents in MDR tumors [8]. Tariquidar analogs, as the third-generation of P-gp inhibitors, act through inhibition of P-gp substrate binding, inhibition of ATP hydrolysis or both [9,10] are the candidate inhibitors to clinical usage. Hitherto, there has been no MDR-inhibiting agent approved for clinical use.

Many 1,4-dihydropyridines (DHPs) are clinically used as calcium channel blockers. According to the structure-activity relationship (SAR) studies of DHPs, replacement of carboxylate esters at C3 and C5

Abbreviations: ABC, ATP-binding cassette; MDR, multi-drug resistance; P-gp, P-glycoprotein; DHP, dihydropyridine; NBD, nucleotid binding domain; DCM, dichloromethane; Rhodamine123, (Rho123)

* Corresponding author at: Biotechnology Research Center, Pharmaceutical Technology Institute, Mashhad University of Medical Sciences, Mashhad, Iran.
E-mail address: Hadizadehf@mums.ac.ir (F. Hadizadeh).

https://doi.org/10.1016/j.bioorg.2019.103156
Received 21 November 2018; Received in revised form 31 May 2019; Accepted 24 July 2019
Available online 29 July 2019
0045-2068/

positions of DHPs with aryl carboxamide groups substantially decreases the cardiovascular effects of these compounds [11]. The neuroprotective activity and antioxidant properties for some derivatives of these compounds have been revealed [12,13]. These bioactive structures were also being explored as vasodilator, bronchodilator, antiatherosclerotic, antitumour and antidiabetic agents [14]. New DHP derivatives have also been proposed to reverse MDR [15,16]. *In silico* methods are applied to distinguish important functional groups for increasing the potency and pharmacodynamic effects of synthetic compounds/drug candidates [17–19]. The pharmacokinetic features such as Log p value should not be ignored [20,21]. Increasing the efficacy of chemotherapy can be achieved by reducing the required dose of anticancer agents. For this purpose, MDR pumps are major targets to be inhibited. New synthetic 1,4-DHP derivatives which contain thiophenyl substituent have been reported in our previous works (compounds 1–7) [22]. In the present study, we synthesized new 1,4-DHP derivatives and evaluated them using *in silico* and *in vitro* assays for antitumor and P-gp inhibitory activity.

2. Material and methods

Phenylthioacetone (ChemCruz), 3-nitrobenzaldehyde (Titrachem), 3-chlorobenzaldehyde and acetoacetanilide (Sugma-Aldrich) were purchased and were used without further purification.

2.1. Synthesis

3-Chloro benzaldehyde (0.6 mmol, 70 µl), phenylthioacetone (0.6 mmol, 0.10 g), methyl aminocrotonate (0.6 mmol, 0.07 g) and carbonate ammonium (1.2 mmol, 0.1 g) were added to ethanol solvent and the resulting mixture was refluxed at 72 °C for 20 h. The solvent was removed in vacuum and the remaining materials were dissolved in dichloromethane (DCM). After washing with water in a decanter funnel and drying by Na_2SO_4, the reaction mixture was separated by column chromatography on silica gel eluted with a gradient of ethyl acetate-hexane. Crystallization was carried out by means of these solvents. This reaction was repeated with 3-nitrobenzaldehyde and 3-cyanobenzaldehyde (products **8, 9** and **10**) (see Scheme 1).

3-Nitrobenzaldehyde (0.6 mmol, 0.09 g), phenylthioacetone (0.6 mmol, 0.10 g), acetoacetanilide (0.6 mmol, 0.1 g) and carbonate ammonium (1.8 mmol, 0.14 g) were added to ethanol and the mixture was refluxed at 72 °C for 20 h. Work-up and purification steps were carried out as mentioned above (compound **11**). Melting point ranges, TLC and NMR analyses (supplementary file) showed that purities of these synthetic compounds (≈98%) were adequate for using them in biological tests.

2.2. Biological evaluation

2.2.1. Cell lines

Human gastric carcinoma cell line EPG85-257P and its drug-resistant subline EPG85-257RDB which over expresses P-gp as a result of continuous exposure to anticancer drug were cultured in RPMI-1640 medium supplemented with 10% fetal bovine serum (Gibco, Invitrogen, Paisely, UK), penicillin (100 units/mL) and streptomycin (100 µg/mL) for desired growth, in a humidified incubator at 37 °C in an atmosphere of 5% CO2. DMEM medium (Caisson, USA) was used instead of RPMI-1640 medium for Human umbilical vein endothelial cells (HUVECs) as normal cell line. These cell lines were obtained from the Biotechnology laboratory stocks, Biotechnology Research Center (Mashhad, Iran).

2.2.2. Flow cytometric efflux assay

12-well microplates were harvested and seeded at a density 2×10^5 EPG85-257RDB (one well for EPG85-257P) cells in each well and were incubated for 24 h at 37 °C. Then Rho123 (10 µM) was added to each well and incubated for 45 min. After addition new compounds and verapamil (positive control) at a final concentration of 5 and 15 µM, the cells were further incubated for 30 min at 37 °C. Cells were washed two times with PBS and harvested by trypsinization. After centrifugation, supernatants were removed and cells were re-suspended in ice-cold PBS. Samples were analyzed by a BD FACS Calibur Flow Cytometry System (BD Biosciences, San Jose, USA). Excitation and emission wavelengths were 488 and 530 nm, respectively. Fluorescence intensity of Rho 123 accumulated in the cells was measured.

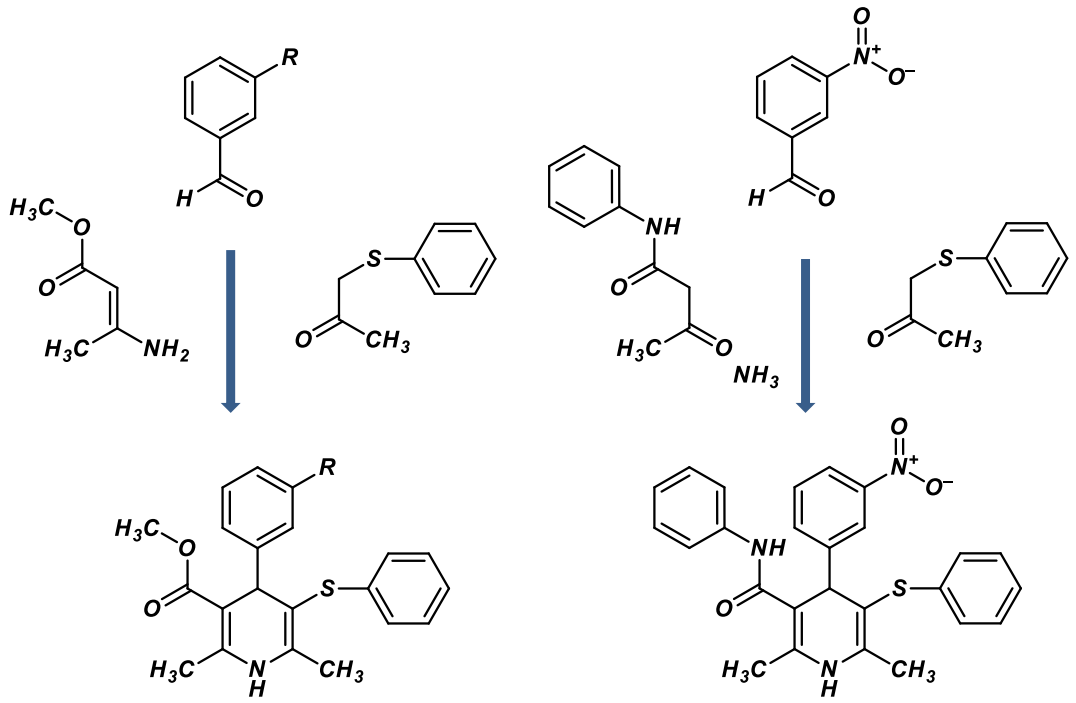

Scheme 1. Syntheses of new DHP derivatives containing thiophenyl moiety based on Hantzsch reaction. (Compounds 8–10 (left) and compound 11 (right), R = NO_2, Cl, CN).

Mean fluorescence intensity (MFI) can be calculated based on Eq. (1).

$$\mathrm{MFI} = \frac{fluorescence\ \ of\ \ test\ \ group(Rho + DHP) - fluorescence\ \ of\ \ blank}{fluorescence\ \ of\ \ control\ \ group(Rho) - fluorescence\ \ of\ \ blank} \quad (1)$$

2.2.3. MTT assay

The cell viability for normal, parental and resistant cell lines was determined in the MTT assay which is the base on reducing the MTT reagent to formazan via mitochondrial dehydrogenases in viable cells.

2.2.3.1. Cytotoxicity of the DHPs. The cell viability of the new compounds in both cell lines (the P-gp expressing and the non-expressing cell line) has been investigated. Both cell lines were harvested and seeded at a density of 5×10^3 cells/well in flat-bottom 96-well plates and incubated for 24 h at 37 °C. New compounds were added to each well at a final concentration of 5 and 15 μM, after 72 h these medium were removed and cells were washed with PBS then MTT reagent (5 mg/ml) was added to each well, after 4 h cell viability was measured by spectrophotometric method. Excitation and emission wavelengths were 550 and 630 nm, respectively. HUVEC*s* cells as normal cell line (with DMEM medium) were used to evaluate cytotoxic effect of new DHPs.

2.2.3.2. Doxorubicin IC_{50}. Both cell lines (parental and resistant) were harvested and seeded at a density of 5×10^3 cells/well in flat-bottom 96-well plates and incubated for 24 h at 37 °C. Doxorubicin was added with different concentrations from 0.1, 0.3, 0.7, 1.5, 5, 10, 15, 20, 25 and 30 μM to each well, after 72 h these medium were removed and cells were washed with PBS then MTT reagent (5 mg/ml) was added to each well, after 4 h cell viability was measured by spectrophotometric method.

2.2.3.3. Co-treatment with doxorubicin and MDR reversal assay. Cell viability assay was performed on P-gp-expressing EPG85-257RDB cell line which was harvested and seeded at a density of 5×10^3 cells/well in flat-bottom 96-well plates and incubated for 24 h at 37 °C. New compounds (also verapamil) at 15 μM and doxorubicin with concentration ranging (0.1, 0.3, 0.5, 0.7, 1.2, 1.5 μM) were added to each well; after 72 h the medium was removed and cells were washed with PBS. Afterwards, MTT reagent (5 mg/ml) was added to each well and cell viability was measured after 4 h using spectrophotometric method.

2.2.4. Flow cytometric cell cycle analysis

For cell cycle analysis, EPG85-257RDB cells were seeded at a density of 4×10^4 cells/well in 24-well plates and incubated for 24 h at 37 °C in the presence of 5% CO2. Then the medium was changed by new medium containing 5 μM of new compound alone (compound **11**) or in combination with 1.5 μM of doxorubicin. Positive control was treated with verapamil (5 μM) as standard P-gp inhibitor. After 24 h, the medium was replaced with fresh medium and the cells were incubated for 48 h at 37 °C in 5% CO2. Then, the cells were washed twice with PBS and harvested by trypsinization. After centrifugation, cells were re-suspended in 300 μl *PI/Triton X-100* (0.05 mg/ml) and incubated for 30 min at 37 °C. Protected samples from light at + 4 °C for 90 min, were evaluated by a BD FACS Calibur Flow Cytometry System (BD Biosciences, San Jose, USA) and analyzed by Flowjo 7.6.1 software.

2.3. In silico methods

2.3.1. Molecular docking

Using molecular docking analysis and experimental studies, Ferreira et al. showed that P-gp has two substrate-binding sites for H (Hoechst 33342) and R (rhodamine-123), and one inhibitor binding M (modulator) site [23,24]. Mouse crystallographic structure for P-gp (PDB: 3G60) was downloaded from the Protein Data Bank and used for this study after applying the following refinement. The DBP (drug binding pocket) of P-gp is almost 100% identical between mouse and human, thereby allowing the use of mouse protein for investigations [25]. AutoDock Tools (ADT) 1.5.6 was utilized to construct the protein and ligand files. All water molecules were removed and polar hydrogens were added to the original crystallographic protein file, and Gasteiger charges were applied. The active site of the protein was defined around the co-crystalized modulator (QZ59-RRR) that has been reported as the modulator site (M site) [24] so grid box dimensions were set to $50 \times 50 \times 50$ Å with grid center (x = 19.3, y = 52.68, z = −0.1) which was used as a setting tool to compute the grid maps. Docking calculations were performed with 2,500,000 energy evaluation and 50 runs using Lamarckian genetic algorithm. Compound 11, as a potent compound, was docked into the drug binding site of the protein via the mentioned grid box using AutoDock 4.2 software [26]. The docked complex was employed for molecular dynamic studies.

2.3.2. Bilayer and ligands parameters

MD simulation was performed using the package GROMACS 5.1, in conjunction with the GROMOS 53a6 force field for protein [27]. PRODRG server that generates a variety of refined parameters for molecules was used to prepare topology and coordinate files for the compound 11 whose chemical structure was drawn and minimized using Discovery Studio Accelry software. We downloaded the DPPC128.pdb file from the website of Peter Tieleman's Biocomputing Group at the University of Calgary in Canada, then replicated the 128 DPPC bilayer to obtain a bilayer of 512 lipids that was suitable for a large membrane protein [28]. The protein ligand complex was placed in the DPPC bilayer using *Princ* command and rotated using the *rotate* command in GROMACS so that its long axis was perpendicular to the lipid surface. The Inflate GRO method was used for packing lipids around the embedded protein [28] (Fig. 1). Using this script, the lipid position was scaled by a special factor; after 26 scaling iterations, a suitable area per lipid was obtained.

2.3.3. Simulation parameters

The generic equilibrated 3-point (SPC216) water model was used to describe the solvent water in the simulation, using the *genbox* command in GROMACS, and chloride ions were added to neutralize the overall charge of the system. Energy minimizations were carried out using the steepest-descent algorithm. Simulations used the NPT ensembles with Parrinello-Rahman pressure coupling (semi-isotropic) to 1 bar and Nose-hoover temperature coupling to 323K. Simulation was performed with full periodic boundary conditions (PBC). MD simulation was performed for a time period of 100 ns for the structure. Long-range electrostatic interactions were computed using the particle mesh Ewald (PME) method. Cut-off 1.2 Å to compute short-range electrostatic and short-range van der Waals interactions was used. The LINCS algorithm was utilized to constrain the lengths of covalent bonds to hydrogen.

3. Result

3.1. Synthesis

*3.1.1. Methyl4-(3-nitrophenyl)-5-(phenythio)-2,6-dimethyl-1,4-dihydropyridine-3carboxylate (**8**)*

Yellow-orange solid; yield (63%, 0.15 g); mp.140–142 °C; ^{1}H NMR (300 MHz, $CDCl_3$): δ = 7.96 (s, 1H, CH), 7.89 (d, J = 8.1 Hz, 1H, CH), 7.45 (d, J = 7.5 Hz, 1H, CH), 7.25(t, J = 7.8 Hz, 1H, CH), 7.06 (m, 5H, CH), 5.63 (s, 1H, NH), 4.53 (s, 1H, CH), 3.45 (s, 3H, OCH_3), 2.34(s, 3H, CH_3), 2.07(s, 3H, CH_3); ^{13}C NMR (75 MHz, $CDCl_3$): δ = 167.82, 149.23, 146.24, 139.19, 136.02, 134.29, 128.95, 128.53, 126.92, 125.92, 125.46, 122.95, 121.46, 100.06, 50.91, 46.14, 20.16, 18.13.

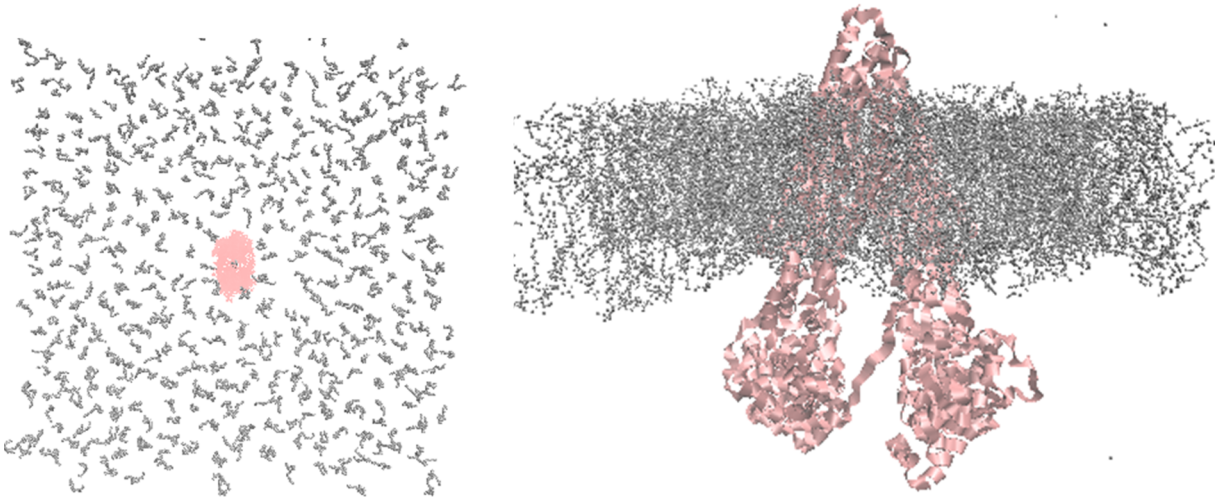

Fig. 1. Packing lipids around the embedded protein-ligand complex via the Inflate GRO method.

*3.1.2. Methyl4-(3-chlorophenyl)-5-(phenythio)-2,6-dimethyl-1,4-dihydropyridine-3-carboxylate **(9)***

White solid; yield (48%, 0.11 g); mp.148–151 °C; ^{1}H NMR (300 MHz, $CDCl_3$): δ = 7.06 (m, 9H, CH), 5.52 (s, 1H, NH), 4.37 (s, 1H, CH), 3.45 (s, 3H, OCH_3), 2.32(s, 3H, CH_3), 2.05 (s, 3H, CH_3); ^{13}C NMR (75 MHz, $CDCl_3$): δ = 168.07, 149.13, 145.82, 138.89, 136.63, 133.58, 128.96 (d), 128.09, 126.41 (d), 125.14, 106.11, 99.50, 50.83, 45.84, 20.12, 18.11.

*3.1.3. Methyl4-(3-cyanophenyl)-5-(phenythio)-2,6-dimethyl-1,4-dihydropyridine-3-carboxylate **(10)***

Yellow solid; yield (60%, 0.135 g); mp.147–150 °C; ^{1}H NMR (300 MHz, $CDCl_3$): δ = 7.42 (s,1H, CH), 7.34 (m,2H, CH), 7.18 (m, 2H, CH), 7.06 (m, 4H, CH), 5.61 (s, 1H, NH), 4.43 (s, 1H, CH), 3.44(s, 3H, OCH_3), 2.33(s, 3H, CH_3), 2.04(s, 3H, CH_3); ^{13}C NMR (75 MHz, $CDCl_3$): δ = 166.82, 147.57, 145.21, 138.15, 135.08, 131.57, 130.73, 128.93, 127.92, 127.47, 125.73, 124.37, 118.43, 110.83, 103.03, 98.98, 49.86, 44.95, 19.04, 17.01.

*3.1.4. 5-(phenylthio)-2,6-dimethyl-4-(3-nitrophenyl)N-phenyl-1,4-dihydropyridine-3-carboxamide **(11)***

yellow solid; Yield (62%, 0.17 g); mp.191–192 °C; ^{1}H NMR (300 MHz, $CDCl_3$): δ = 8.21(s,1H, CH),8.09 (d, J = 8.1 Hz, 1H, CH), 7.66 (d, J = 7.8 Hz, 1H, CH),7.46(t, J = 7.8 Hz, 1H, CH),7.13(m, 10*H*, CH), 6.81 (s, 1H, NH), 5.65 (s, 1H, NH), 4.55 (s, 1H, CH), 2.45(s, 3H, CH_3), 2.19(s, 3H, CH_3); ^{13}C NMR (75 MHz, $CDCl_3$): δ = 166.40, 149.75, 146.34, 142.75, 140.13, 137.84, 136.01, 133.86, 129.43, 128.99, 126.75, 125.60, 124.09, 122.84, 122.39, 119.84, 104.15, 100.56, 47.50, 19.39, 18.29.

3.2. Biological evaluations

3.2.1. Flow cytometric efflux assay

The fluorescent dye Rho123 is a well-known reference P-gp substrate used to characterize the P-gp inhibitory potential of compounds [3]. Rho123 accumulation assay in the resistant cell line (EPG85-257RDB) showed that the synthetic DHP derivatives increased intracellular Rho123 accumulation significantly, as compared to the negative control (cell treated with Rho alone). Moreover, flow cytometry results, based on calculated mean fluorescence intensity (MFI) (Eq. (1)), showed that cells treated with these asymmetric DHPs had about 2–3 folds higher accumulation of Rho123 in comparison with verapamil as a positive control (Figs. 2 and 3).

The calculated MFI for the combination of Rho with verapamil, compound 8, 9, 10 and 11 were 2.2 ± 0.35, 6.1 ± 0.33, 3.6 ± 0.33, 5 ± 0.16 and 4.46 ± 0.45 respectively at15 μM (Fig. 2) while all of compounds were weaker than that of verapamil at 5 μM.

3.2.2. MTT assay

Cell viability of the DHP compounds and verapamil were evaluated in the resistant and normal cell lines using MTT assay.

3.2.2.1. Cytotoxicity of DHP compounds in normal cell line. Cell viability assay in the normal cells line (HUVEC) showed that there was no cytotoxic effect of DHP derivatives at 5 μM concentration following 72 h of incubation. The cell viability remained at about 100% for all of the tested compounds (Fig. 4). Moreover, increasing the concentration of compounds from 5 to 15 μM revealed a decline in the viability of normal cells to 90% for compound 11 while the rest of compounds did not have any cytotoxic effect (Fig. 4).

3.2.2.2. Cytotoxicity effects in cancer cells. The results of MTT assay in resistant cells indicated that the cell viability was significantly reduced to about 70–94% in the presence of different structures of DHPs at 5 μM following 72 h incubation (Fig. 5).

At 15 μM concentration, compound 11 demonstrated the highest cytotoxicity effects on resistant and normal cell lines. Compound 8 showed a potent cytotoxicity effect on the resistant cells while showing no toxic effect on normal cells. Compounds 10 had weaker cytotoxicity effects on resistant and normal cells especially at the low concentration of 5 μM. Cytotoxic effect of compounds at 15 μM concentration was lower in the parental versus resistant cell line as shown in Table 1. According to Table 1 the concentration of the DHP compounds is equal in both parental and resistant cell lines (15 μM), but the cell viability in the parental cell line is more than the resistant cell line by use of DHP compounds.

3.2.2.3. Doxorubicin IC_{50}. The calculated IC_{50} values of the doxorubicin in resistant (9 μM) EPG85-257RDB and parental (0.1 μM) EPG85-257P cells were different. This is expected according to the P-gp-dependent efflux phenomenon which reduces intracellular accumulation of doxorubicin (Fig. 7).

3.2.2.4. Cell viability of the resistant cells in combination with doxorubicin &MDR reversal

3.2.2.4.1. Cell viability of the resistant cells in combination with doxorubicin. Co-administration of synthetic DHPs (at 15 μM) and doxorubicin (0.7 μM) showed a reduction in the viability of resistant cells to 20.5% ± 3.58, 39.2% ± 4.82, 54% ± 3.72 and 74.61% ± 6.15 for compounds 11, 8, 9 and 10 respectively (Fig. 6).

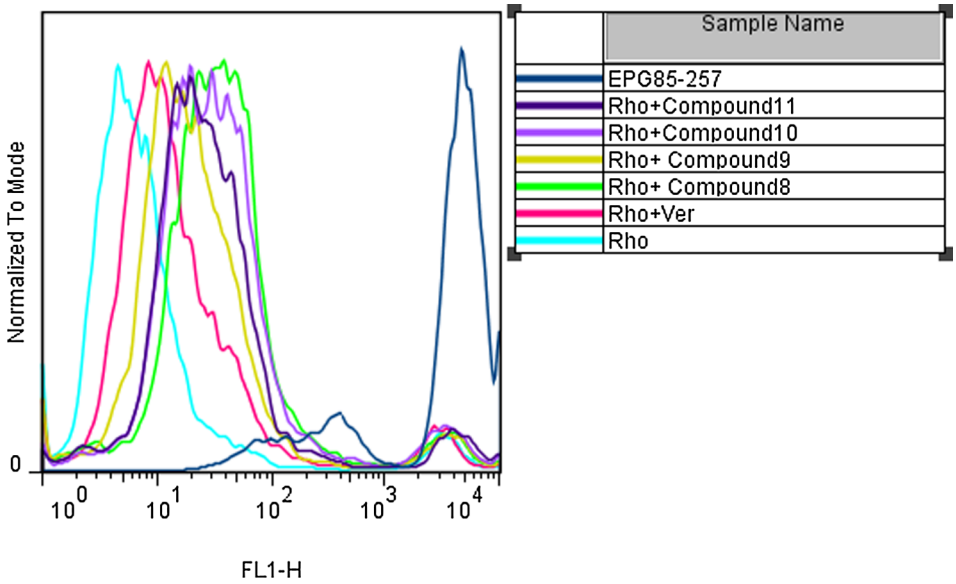

Fig. 2. Flow cytometry results of efflux assay for cells treated with Rho dye (as negative control), Rho + verapamil (15 μM) (as positive control) and Rho + DHP compounds (15 μM).

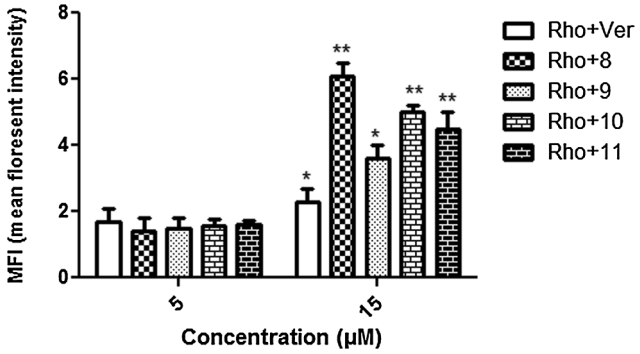

Fig. 3. The MFI results are presented as the n = 3, mean ± SD: *P < 0.05; **P < 0.01; ***P < 0.001.

Compound 10 alone had negligible effects on the viability of resistant (and normal) cells and could be considered for decreasing IC_{50} value of doxorubicin in the MDR reversal assay. Because of having two biological effects, other compounds could not be selected to show differences of IC50 values in MDR reversal assay.

3.2.2.4.2. MDR reversal assay. Results could reveal the effect of inhibitor in restoring the anticancer drug activity in MDR.

The MTT test as MDR reversal assay was applied to evaluation the sensitivity to doxorubicin which was enhanced via DHP derivatives. We selected compound 10 because of containing the least toxic effect of this compound on resistant cells when it was used alone. Co-administration of doxorubicin with compound 10 at 15 μM reduced the IC_{50} from 9 μM to 1.5 μM in the resistant cell line (Fig. 7).

3.2.3. Apoptosis

Propidium iodide (PI) is used to stain DNA contents that indicate apoptotic cells in cell cycle analysis [29]. Cell cycle profiles were monitored by flow cytometric analysis for DNA content in the presence of verapamil and synthetic compound 11 as the potent compound based on Fig. 6 containing two biological effects (cytotoxicity on cancer cell and P-gp inhibitory activity) in combination with doxorubicin. Sub-G1 peak representing the subpopulation of apoptotic cells in each sample is shown in Fig. 8. DNA content histograms vs FL2-H showed pick area for untreated cells (as control) 8.56%, doxorubicin alone 14.5%, verapamil alone 17.7%, compound **11** alone 20.4%, combination of doxorubicin and verapamil 34%, and combination of doxorubicin and compound **11** 45.3% (Fig. 8).

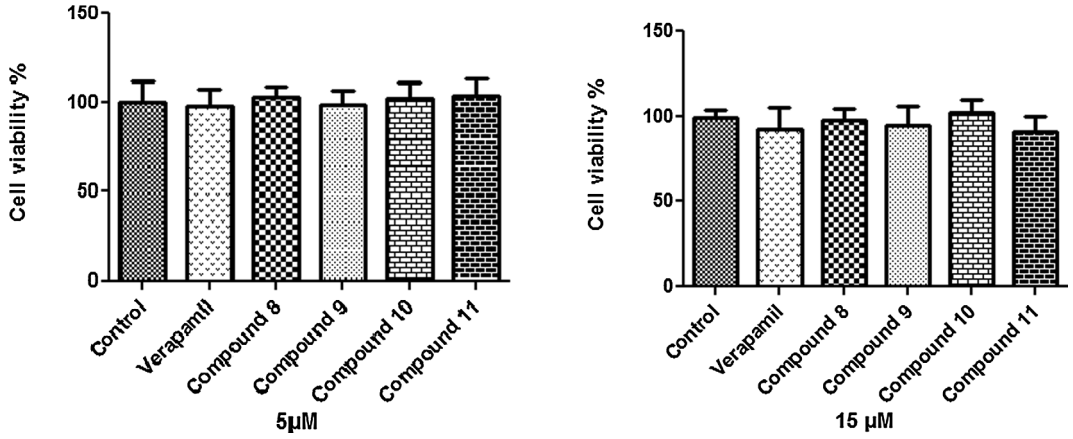

Fig. 4. Cytotoxicity of the DHP derivatives at 5 (left) and 15 (right) μM in normal cell line in 72 h. (n = 3, mean ± SD).

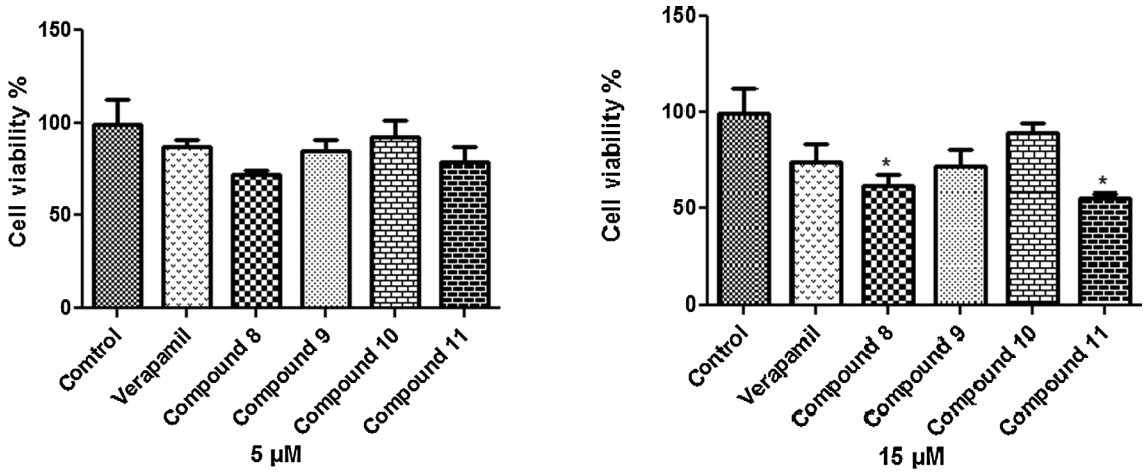

Fig. 5. Cytotoxicity effect of DHPs with 5 (left) and 15 µM in resistant cells (right) in 72 h. Untreated cell was used as control (n = 3, mean ± SD: *P < 0.05; **P < 0.01; ***P < 0.001). At 15 µM concentration, compound11 demonstrated the highest cytotoxicity effect.

3.3. In silico method

The protein-ligand binding affinity can be calculated using Autodock program via molecular docking approach. The binding scores, as an index used for the estimation of binding affinity of the protein and ligands, were −8.3 and −9.12 kcal/mol for verapamil and compound 11, respectively. The negative score indicates high affinity and the capacity of forming stable complexes. Discovery studio software was used to visualize the active site.

As shown in Fig. 9 compound 11 is stabilized by adjacent hydrophobic residues PHE332, LEU335, ILE336, PHE339, PHE724, PHE728, LEU971, PHE974 and VAL978, which are present in the active site. Moreover, the phenyl ring of Phe728 forms a π-π stacking interaction with the phenyl ring attached to the amide group of compound 11. An

Table 1
The structure of new synthesized DHPs, MFI and %cell viability of three cell lines (in the presence of 15 µM DHP).

compound	Structure of synthesized DHPs	MFI	%Cell viability (Parental cells EPG85-257P)	% Cell viability (resistant cells EPG85-257RDB) Doxorubicin Combination	% Cell viability (normal cells HUVEC)
8	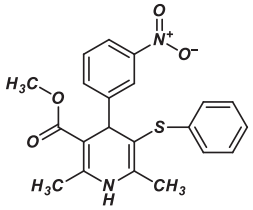	6.1 ± 0.33	75 ± 8.10	61.40 ± 4.79 39.24 ± 4.82	97.30 ± 5.87
9	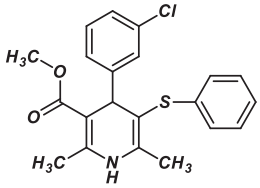	3.6 ± 0.33	81 ± 5.61	72.45 ± 6.72 54.01 ± 3.74	94.33 ± 9.28
10	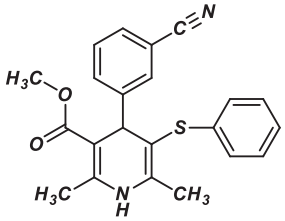	5 ± 0.16	94 ± 1.8	89.06 ± 4.51 74.61 ± 6.15	102.35 ± 6.03
11	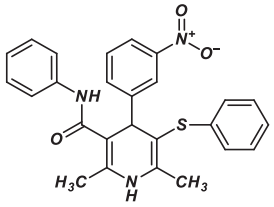	4.46 ± 0.45	67 ± 7.1	55.5 ± 1.90 20.53 ± 3.58	90.94 ± 7.58

Viability of resistant cells was determined in the presence of 15 µM DHP alone (as an inhibitor) and in combination with DOX 0.7 µM. Data were analyzed using GraphPad Prism 5.0 software and were presented as mean ± SD (n = 3).

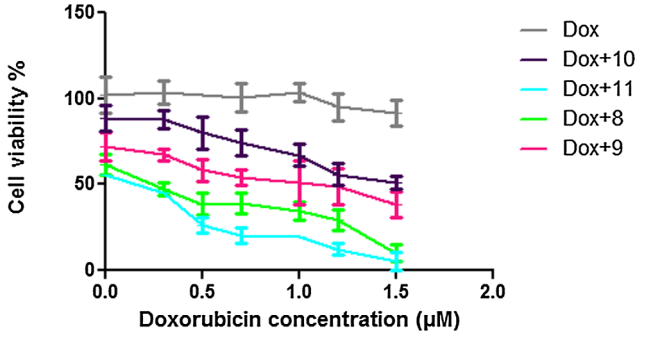

Fig. 6. Cell viability in the resistant cell line treated with synthetic DHPs (15 μM) in combination with different concentrations of doxorubicin (μM) following a 72-h incubation. Each point represents the mean ± SD, n = 3.

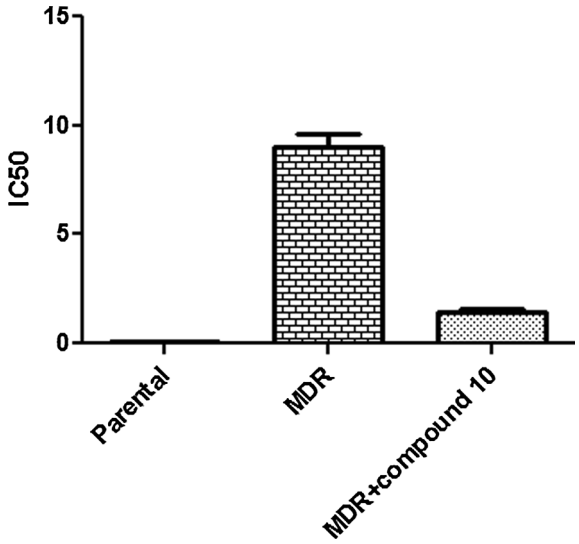

Fig. 7. IC_{50} of doxorubicin was about 0.1 μM and 9 μM in parental and resistant cell lines, respectively, following 72 h incubation. Combination of doxorubicin and compound 10 (15 μM) reduced the IC50 from 9 μM to 1.5 μM.

intra-ligand π-π stacking interaction is formed between the two remaining phenyl groups of the compound. Another π-π stacking interaction between phenyl groups of Tyr303 and Tyr306 is shown in Fig. 9. While there is no electrostatic interaction between the compound and residues at drug binding site, hydrogen bond interactions are present between residues at drug binding site such as SER975 - PHE 974 - LEU971 and SER 725 - SER 729 that could change in the simulation time.

As shown in Fig. 10 compound 11 is stabilized by nearby hydrophobic residues MET68, PHE332, LEU335, ILE336, PHE339, PHE728, PHE974, VAL978 and ALA981 in the active site. Additionally, one π-π-δ interaction is formed between the two phenyl groups of the compound 11 and LEU336. The carbonyl group of compound 11 interacted with SER975 to form a hydrogen bond (1.9 Å). This electrostatic interaction can be seen before starting dynamic and is not detected in docking process. Intrarmolecular interaction forms another hydrogen bond inside SER 975(OH…CO). Residues such as PHE 339-LEU335 and PHE332-LEU336 observed at drug binding site can form other hydrogen bonds around compound 11.

After 45 ns simulation, compound 11 is stabilized by nearby hydrophobic residues MET68, PHE310, VAL327, PHE331, PHE332, LEU335, ILE336, PHE339, ALA950, PHE974 VAL978, ILE977, PHE979, GLY980, ALA981 and MET982 at the active site. Moreover, the two phenyl rings of the compound 11 interact with PHE339 through π-π-π stacking. NH group of compound 11 forms a cation-π interaction with the phenyl ring of Phe974. Hydrogen binding is preserved between the carbonyl group of compound 11 and SER975 with decreasing distance from 1.9 Å to 1.5 Å. Another hydrogen bond can be seen between NO2 group of the compound and ALA981 (distance;1.8 Å). Residues such as PHE332-LEU336, ALA951-TYR113, TYR949-GLY980, THR314-TRP311 and PHE979-MET980 are observed at drug binding site to form hydrogen bond interactions (see Fig. 11).

After 100 ns simulation compound 11 was stabilized by nearby hydrophobic residues MET68, PHE71, ALA307, PHE310, PHE331, PHE332, LEU335, ILE336, PHE339, ALA950, PHE974 and VAL978, PHE979, GLY980, ALA981. Additionally, the phenyl group attached to the amide moiety of compound 11 forms π-π interaction with the phenyl ring of PHE310 while another π-π interaction is formed between the two remaining phenyl groups of the compound. The hydrogen binding is preserved between NO2 group of the compound and ALA981 in this simulation time (distance; 2 Å). Another hydrogen bond is observed between NO2 group and PHE979 with a distance of 3.3 Å Hydrogen bonds between residues such as PHE332-LEU336, ALA307-TYrp311 and THR314-PHE310 can be found at drug binding site (see Fig. 12).

4. Discussion

Recent studies on the physiological effects of DHP derivatives have demonstrated the ability of these compounds to revers chemotherapy resistance besides exerting antitumor effects [15].

In the present study, flow cytometry findings showed that new DHPs (at 15 μM) increased intracellular concentration of Rho 123 by about 2–3 folds compared with verapamil as a standard P-gp inhibitor. The accumulation of Rho123 in the resistant cells by DHP analogs at 15 μM suggest that they could modulate the P-gp functional activity, thereby reducing the P-gp mediated efflux of Rho123 in the resistant cells. The increasing of Rho123 accumulation by these compounds at 5 μM is equal or weaker than verapamil that indicates the potency for inhibiting efflux process at low concentration of DHPs is not considerable so at the lower concentration (5 μM) this inhibitory potential of DHPs is diminished.

Reduced cell viability in the tested cancer cell line by MTT assay especially at the longer incubation time point (72 h) can be related to the antitumor activity [30–32]. The tested compounds had cytotoxicity effect (antitumor effects) in resistant and parental cancer cell lines but were devoid of any toxic effect on normal cells. In previous studies reporting low cytotoxic effects, duration of incubation was mainly 48 h rather than 72 h [30,33].

Combination of the compounds with doxorubicin was also evaluated via MTT assay and cell cycle analysis. The main anticancer action of doxorubicin has been suggested to be mediated by free radical generation and, particularly, topoisomerase II inhibition [34]. It has also been mentioned that resistant tumor cells do not respond to chemotherapy because of the efflux of anticancer drugs by overexpressed of P-gp transporter. Therefore, the efficiency of anticancer drugs could be enhanced by combination with the pump inhibitor in resistant tumor cells. In this study, the effect of combination treatment with DHP compounds and doxorubicin was tested using MTT assay. The response of resistant cancer cells to doxorubicin was improved in the presence of DHP as an efflux pump inhibitor. More potent compound such as 11 could act via two MDR inhibitory and cytotoxicity (antitumor) effects on resistant cancer cells and had toxic effect on normal cells (10%) after 72 h of incubation. Fig. 4 shows that the cell viability of normal cell line (HUVEC) was decreased by compound 11 more than compound 8, so this mentioned compound (11) can also be replaced with compound 8 (15 μM) which lacks toxic effect on normal cells.

To report IC_{50} and the sensitivity to doxorubicin, the resistant cell line was compared with the parental cell line. In this evaluation, compound 10 reduced the IC_{50} of doxorubicin in the resistant cell line from 9 to 1.5 μM while this compound lacked any cytotoxicity or

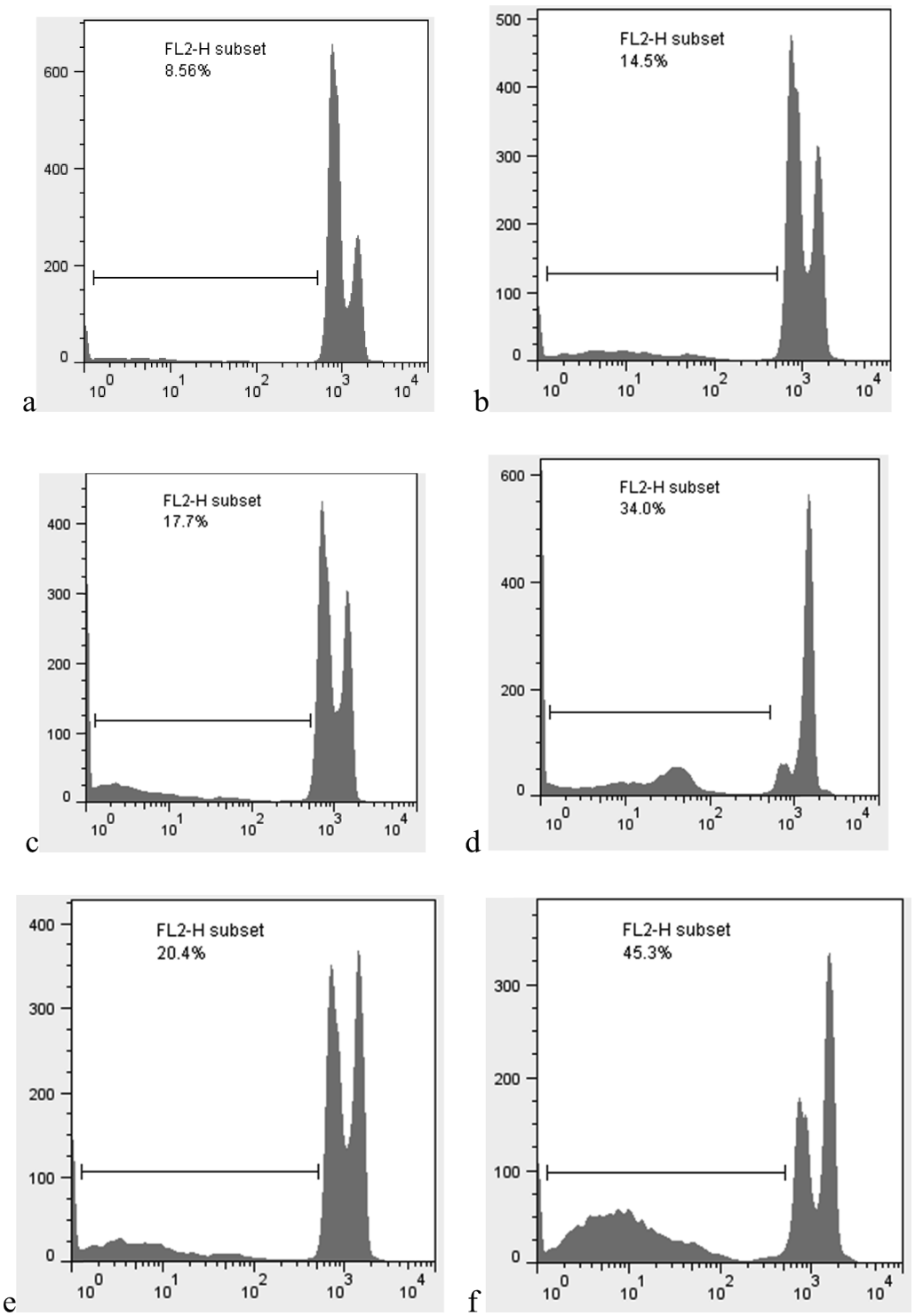

Fig. 8. Flow- cytometric analysis for DNA content. Sub-G1 peak representing the subpopulation of cell related percentage of apoptotic cells **(a)** control, (**b)** doxorubicin, (**c)** verapamil, (**d)** doxorubicin + verapamil, (**e)** compound **11**, (**f**) doxorubicin + compound **11** in (5 μM) in 72 h.

antitumor effect on resistant cells when used alone.

Apoptosis can be induced by a wide variety of factors [32] including chemotherapeutic agents [35]. In this research doxorubicin was used as an anticancer agent that can induce apoptosis [36]. We were able to indicate that the pro-apoptotic effects of doxorubicin are improved in the presence of new synthetic DHPs or verapamil as a p-gp inhibitor. Sub-G1 peak representing the proportion of apoptotic cells showed 34% and 45% apoptosis in the cells treated with doxorubicin + verapamil and doxorubicin + compound 11, respectively. This suggests the potential utility of DHP (compound 11) as a standard adjunct to enhance the pro-apoptotic effects of doxorubicin (even at low concentration 5 μM).

The ligand-protein interactions of mouse, rat and human P-gp derived from molecular docking studies indicated their similar binding patterns [37]. To obtain exact information about structure and function of membrane proteins such as P-gp, the lipid bilayer should surround protein-ligand complex. Interacting residues at drug binding site as well as the type of binding interactions could be investigated via molecular

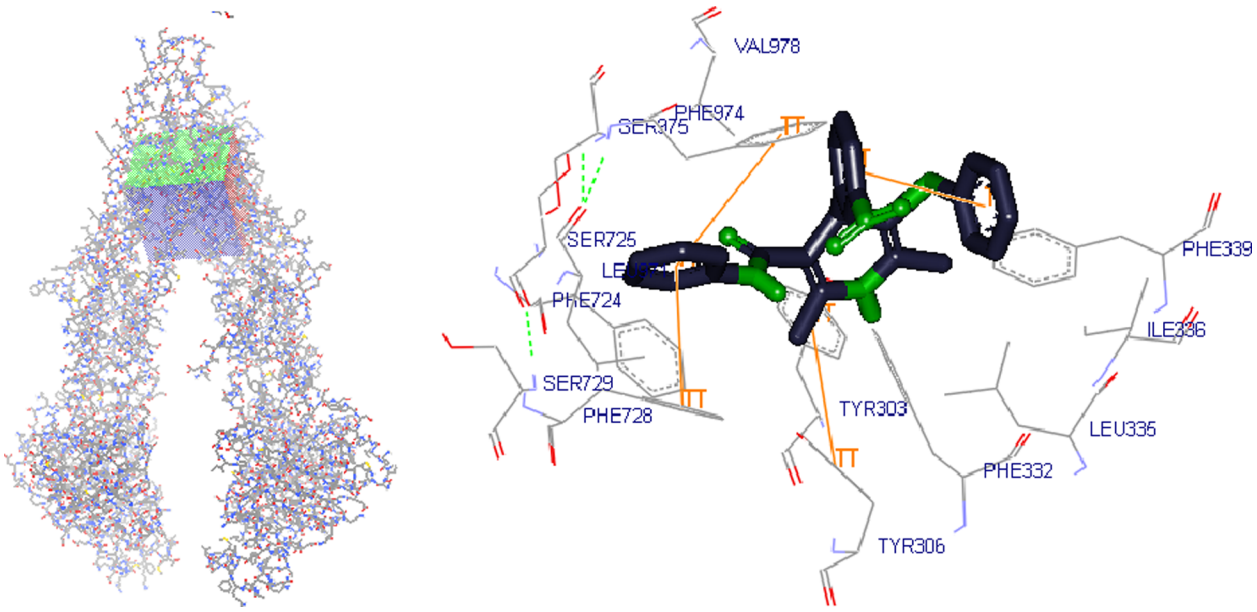

Fig. 9. Defined grid box at drug binding site of the protein (left). Active site of the protein after molecular docking (right).

docking results and trajectory files from MD simulation.

Locating the ligand (compound 11) at drug binding site, which is a hydrophobic area, through molecular docking process causes hydrophobic interactions between ligand and protein without any electrostatic interactions. Packing lipid bilayer around protein-ligand complex following minimization steps causes the appearance of electrostatic interactions between ligand and protein which are preserved in MD simulation time. Increased number of hydrogen bonds between residues at active site from docking process to dynamic steps may be due to the formation of special shapes by aromatic residues and polar residues during conformational changes of the protein through simulation [38,39]. Based on the *in silico* methods, the DHP-P-gp complex is stable enough and DHPs could increase intracellular accumulation of drugs via occupying the drug binding site of P-gp. After binding, DHP will not be displaced by other substrates such as anticancer drug, ensuring a durable inhibition of efflux phenomenon.

5. Conclusions

In the current study, new DHP structures containing thiophenyl substitution were synthesized and showed to possess selective cytotoxicity against tumor cells and enhance the sensitivity of resistant tumor cells to doxorubicin. The findings of efflux assay as well as MDR reversal test and *in silico* modeling revealed that the aforementioned biological effects could be attributed to the inhibition of efflux P-gp pumps. Further studies are encouraged to explore the antitumor potential of these synthetic compounds alone and in combination with doxorubicin in experimental models of tumors.

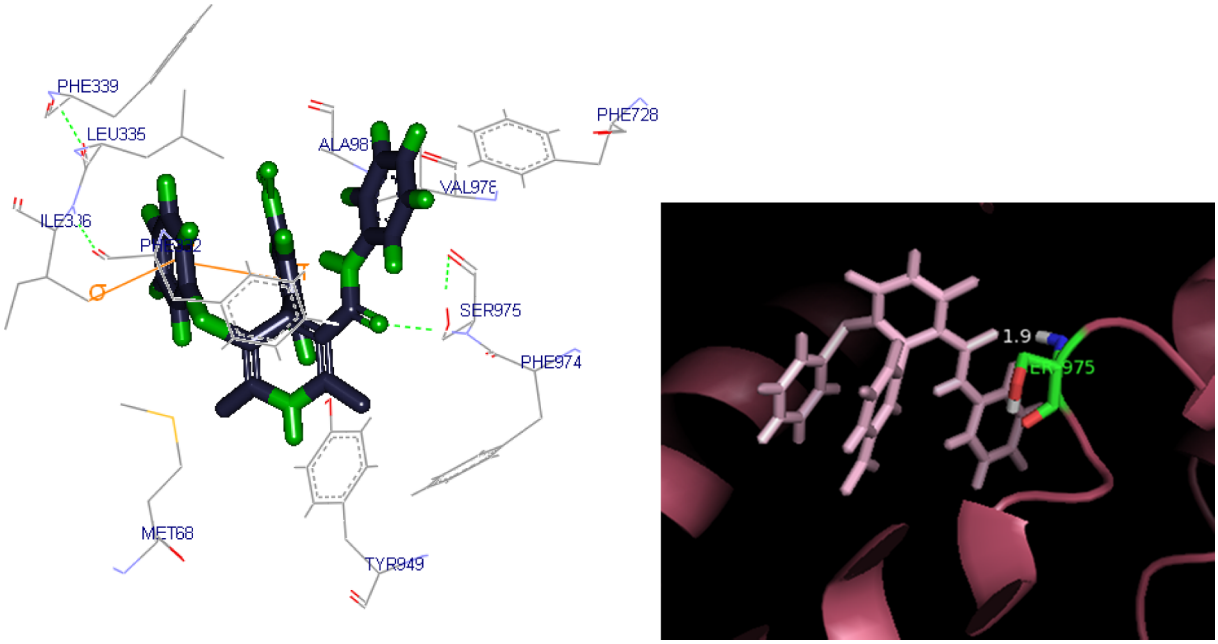

Fig. 10. Active site of the protein after packing lipid bilayer around the protein-ligand complex and minimization steps before MD simulation (left). Distance between SER 975 and carbonyl group of compound 11 was measured with Pymol software (right).

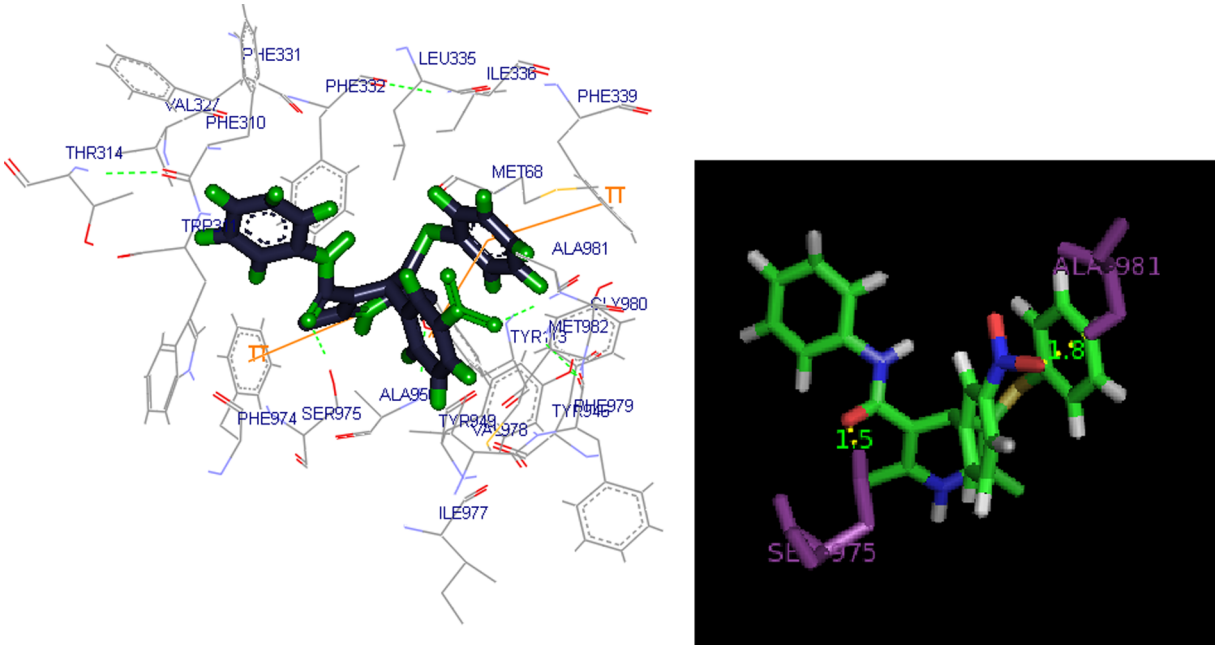

Fig. 11. Active site of the protein after 45 ns MD simulation (left), Distance between SER 975 and carbonyl, ALA981 and NO2 group was measured with Pymol software (right.

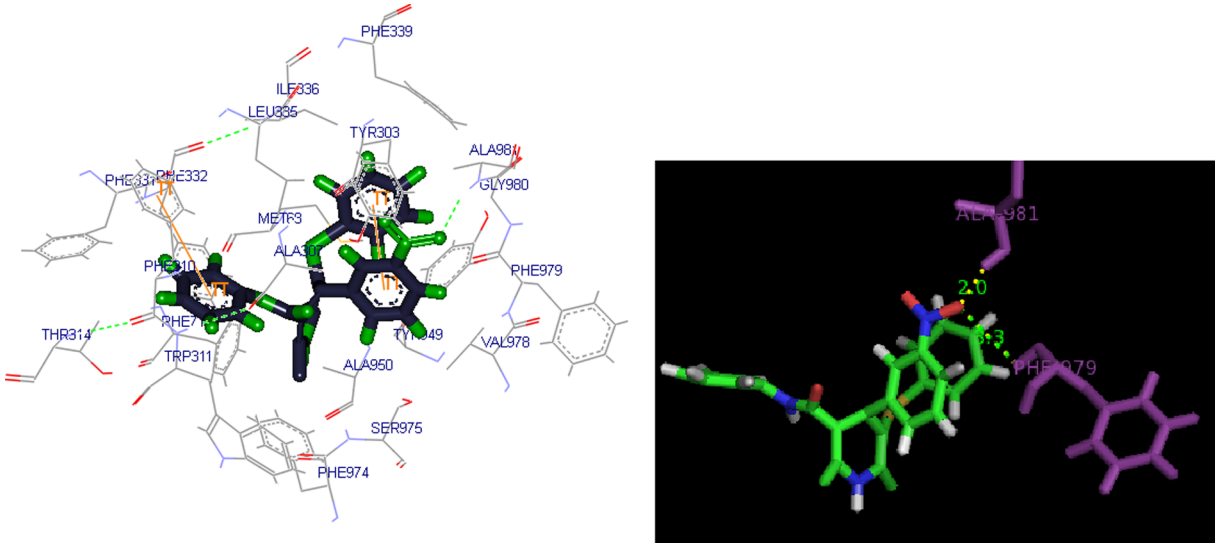

Fig. 12. Active site of the protein after 100 ns MD simulation (left), Distance between NO2 group and PHE979 and ALA981 was measured with Pymol software (right.

Declaration of Competing Interest

The authors have declared no conflict of interest.

Acknowledgement

The financial support by Mashhad University of Medical Sciences, Iran is gratefully acknowledged.

This work was part of Sh. Mollazadeh PhD thesis (grant no. 931452).

Appendix A. Supplementary material

Supplementary data to this article can be found online at https://doi.org/10.1016/j.bioorg.2019.103156.

References

[1] S.V. Ambudkar, I.-W. Kim, Z.E. Sauna, The power of the pump: mechanisms of action of P-glycoprotein (ABCB1), Eur. J. Pharm. Sci. 27 (5) (2006) 392–400.
[2] S. Linn, G. Giaccone, MDR1/P-glycoprotein expression in colorectal cancer, Eur. J. Cancer 31 (7–8) (1995) 1291–1294.
[3] A. Fortuna, G. Alves, A. Falcao, In vitro and in vivo relevance of the P-glycoprotein probe substrates in drug discovery and development: focus on rhodamine 123, digoxin and talinolol, J. Bioequiv. Availab. (2011) 1–23.
[4] K. Katayama, K. Noguchi, Y. Sugimoto, Regulations of P-glycoprotein/ABCB1/MDR1 in human cancer cells, New J. Sci. 2014 (2014).
[5] X. Gu, Y. Jiang, Y. Qu, J. Chen, D. Feng, C. Li, X. Yin, Synthesis and biological evaluation of bifendate derivatives bearing 6, 7-dihydro-dibenzo [c, e] azepine scaffold as potential P-glycoprotein and tumor metastasis inhibitors, Eur. J. Med. Chem. 145 (2018) 379–388.
[6] D. Szöllősi, G. Szakács, P. Chiba, T. Stockner, Dissecting the forces that dominate dimerization of the nucleotide binding domains of ABCB1, Biophys. J. 114 (2) (2018) 331–342.
[7] M.E. Zoghbi, L. Mok, D.J. Swartz, A. Singh, G.A. Fendley, I.L. Urbatsch, G.A. Altenberg, Substrate-induced conformational changes in the nucleotide-binding domains of lipid bilayer-associated P-glycoprotein during ATP hydrolysis,

J. Biol. Chem. (2017) jbc. M117. 814186.
[8] S. Shukla, C.-P. Wu, S.V. Ambudkar, Development of inhibitors of ATP-binding cassette drug transporters–present status and challenges, Expert Opin. Drug Metab. Toxicol. 4 (2) (2008) 205–223.
[9] E. Fox, S.E. Bates, Tariquidar (XR9576): a P-glycoprotein drug efflux pump inhibitor, Expert Rev. Anticancer Ther. 7 (4) (2007) 447–459.
[10] L.D. Weidner, K.L. Fung, P. Kannan, J.K. Moen, J.S. Kumar, J. Mulder, R.B. Innis, M.M. Gottesman, M.D. Hall, Tariquidar is an inhibitor and not a substrate of human and mouse P-glycoprotein, Drug Metab. Dispos. 44 (2) (2016) 275–282.
[11] A. Shah, J. Bariwal, J. Molnár, M. Kawase, N. Motohashi, Advanced dihydropyridines as novel multidrug resistance modifiers and reversing agents, Bioactive Heterocycles VI, Springer, 2007, pp. 201–252.
[12] G. Tenti, J. Egea, M. Villarroya, R. León, J.C. Fernández, J.F. Padín, V. Sridharan, M.T. Ramos, J.C. Menéndez, Identification of 4, 6-diaryl-1, 4-dihydropyridines as a new class of neuroprotective agents, MedChemComm 4 (3) (2013) 590–594.
[13] A. Velena, N. Zarkovic, K. Gall Troselj, E. Bisenieks, A. Krauze, J. Poikans, G. Duburs, 1,4-dihydropyridine derivatives: dihydronicotinamide analogues—model compounds targeting oxidative stress, Oxidative Med. Cell. Longevity 2016 (2016).
[14] S. Ko, M. Sastry, C. Lin, C.-F. Yao, Molecular iodine-catalyzed one-pot synthesis of 4-substituted-1, 4-dihydropyridine derivatives via Hantzsch reaction, Tetrahedron Lett. 46 (34) (2005) 5771–5774.
[15] C. Baumert, M. Günthel, S. Krawczyk, M. Hemmer, T. Wersig, A. Langner, J. Molnár, H. Lage, A. Hilgeroth, Development of small-molecule P-gp inhibitors of the N-benzyl 1, 4-dihydropyridine type: Novel aspects in SAR and bioanalytical evaluation of multidrug resistance (MDR) reversal properties, Bioorg. Med. Chem. 21 (1) (2013) 166–177.
[16] M. Kawase, A. Shah, H. Gaveriya, N. Motohashi, H. Sakagami, A. Varga, J. Molnár, 3, 5-Dibenzoyl-1, 4-dihydropyridines: synthesis and MDR reversal in tumor cells, Bioorg. Med. Chem. 10 (4) (2002) 1051–1055.
[17] B. Wang, L.-Y. Ma, J.-Q. Wang, Z.-N. Lei, P. Gupta, Y.-D. Zhao, Z.-H. Li, Y. Liu, X.-H. Zhang, Y.-N. Li, Discovery of 5-cyano-6-phenylpyrimidin derivatives containing an acylurea moiety as orally bioavailable reversal agents against P-glycoprotein-mediated mutidrug resistance, J. Med. Chem. (2018).
[18] G.E. Jara, D.M.A. Vera, A.B. Pierini, Binding of modulators to mouse and human multidrug resistance P-glycoprotein. A computational study, J. Mol. Grap. Model. 46 (2013) 10–21.
[19] A. Palmeira, E. Sousa, M.H. Vasconcelos, M.M. Pinto, Three decades of P-gp inhibitors: skimming through several generations and scaffolds, Curr. Med. Chem. 19 (13) (2012) 1946–2025.
[20] F. Klepsch, P. Vasanthanathan, G.F. Ecker, Ligand and structure-based classification models for prediction of P-glycoprotein inhibitors, J. Chem. Inf. Model. 54 (1) (2014) 218–229.
[21] S. Mollazadeh, J. Shamsara, M. Iman, F. Hadizadeh, Docking and QSAR studies of 1, 4-dihydropyridine derivatives as anti-cancer agent, Recent Pat. Anti-Cancer Drug Discov. 12 (2) (2017) 174–185.
[22] S. Mollazadeh, F. Moosavi, F. Hadizadeh, M. Seifi, J. Behravan, M. Iman, Synthesis and DFT study on Hantzsch reaction to produce asymmetrical compounds of 1, 4-dihydropyridine derivatives for P-glycoprotein inhibition as anticancer agent, Recent Pat. Anti-Cancer Drug Discov. (2018).
[23] R.J. Ferreira, M.-J.U. Ferreira, D.J. dos Santos, Molecular docking characterizes substrate-binding sites and efflux modulation mechanisms within P-glycoprotein, J. Chem. Inf. Model. 53 (7) (2013) 1747–1760.
[24] S.G. Aller, J. Yu, A. Ward, Y. Weng, S. Chittaboina, R. Zhuo, P.M. Harrell, Y.T. Trinh, Q. Zhang, I.L. Urbatsch, Structure of P-glycoprotein reveals a molecular basis for poly-specific drug binding, Science 323 (5922) (2009) 1718–1722.
[25] H. Min, M. Niu, W. Zhang, J. Yan, J. Li, X. Tan, B. Li, M. Su, B. Di, F. Yan, Emodin reverses leukemia multidrug resistance by competitive inhibition and down-regulation of P-glycoprotein, PLoS ONE 12 (11) (2017) e0187971.
[26] J. Li, B. Duan, Y. Guo, R. Zhou, J. Sun, B. Bie, S. Yang, C. Huang, J. Yang, Z. Li, Baicalein sensitizes hepatocellular carcinoma cells to 5-FU and Epirubicin by activating apoptosis and ameliorating P-glycoprotein activity, Biomed. Pharmacother. = Biomed. Pharmacother. 98 (2018) 806–812.
[27] D. Van Der Spoel, E. Lindahl, B. Hess, G. Groenhof, A.E. Mark, H.J. Berendsen, GROMACS: fast, flexible, and free, J. Comput. Chem. 26 (16) (2005) 1701–1718.
[28] C. Kandt, W.L. Ash, D.P. Tieleman, Setting up and running molecular dynamics simulations of membrane proteins, Methods 41 (4) (2007) 475–488.
[29] C. Riccardi, I. Nicoletti, Analysis of apoptosis by propidium iodide staining and flow cytometry, Nat. Protoc. 1 (3) (2006) 1458.
[30] Y.-S. Li, D.-S. Zhao, X.-Y. Liu, Y.-X. Liao, H.-W. Jin, G.-P. Song, Z.-N. Cui, Synthesis and biological evaluation of 2, 5-disubstituted furan derivatives as P-glycoprotein inhibitors for Doxorubicin resistance in MCF-7/ADR cell, Eur. J. Med. Chem. 151 (2018) 546–556.
[31] Z. Zhang, X. Xiao, T. Su, J. Wu, J. Ren, J. Zhu, X. Zhang, R. Cao, R. Du, Synthesis, structure-activity relationships and preliminary mechanism of action of novel water-soluble 4-quinolone-3-carboxamides as antiproliferative agents, Eur. J. Med. Chem. 140 (2017) 239–251.
[32] H. He, D.-W. Li, L.-Y. Yang, L. Fu, X.-J. Zhu, W.-K. Wong, F.-L. Jiang, Y. Liu, A novel bifunctional mitochondria-targeted anticancer agent with high selectivity for cancer cells, Sci. Rep. 5 (2015) 13543.
[33] R. Hu, J. Gao, R. Rozimamat, H.A. Aisa, Jatrophane diterpenoids from Euphorbia sororia as potent modulators against P-glycoprotein-based multidrug resistance, Eur. J. Med. Chem. 146 (2018) 157–170.
[34] D. Gewirtz, A critical evaluation of the mechanisms of action proposed for the antitumor effects of the anthracycline antibiotics adriamycin and daunorubicin, Biochem. Pharmacol. 57 (7) (1999) 727–741.
[35] F. Yang, S.S. Teves, C.J. Kemp, S. Henikoff, D.N.A. Doxorubicin, torsion, and chromatin dynamics, Biochim. Biophys. Acta (BBA)-Rev. Cancer 1845 (1) (2014) 84–89.
[36] A.G. Patel, S.H. Kaufmann, Cancer: how does doxorubicin work? Elife 1 (2012) e00387.
[37] S. Jain, M. Grandits, G.F. Ecker, Interspecies comparison of putative ligand binding sites of human, rat and mouse P-glycoprotein, Eur. J. Pharm. Sci. (2018).
[38] S. Mollazadeh, A. Sahebkar, F. Hadizadeh, J. Behravan, S. Arabzadeh, Structural and functional aspects of P-glycoprotein and its inhibitors, Life Sci. (2018).
[39] E.E. Chufan, K. Kapoor, S.V. Ambudkar, Drug–protein hydrogen bonds govern the inhibition of the ATP hydrolysis of the multidrug transporter P-glycoprotein, Biochem. Pharmacol. 101 (2016) 40–53.